THE ASTROPHYSICAL JOURNAL, 344:1010–1025, 1989 September 15

A TWISTED FLUX-TUBE MODEL FOR SOLAR PROMINENCES. I. GENERAL PROPERTIES

E. R. PRIEST, A. W. HOOD, AND U. ANZER
Mathematical Sciences Department, University of Saint Andrews
Received 1988 July 1; accepted 1989 January 24

ABSTRACT

It is proposed that a solar prominence consists of cool plasma supported in a large-scale curved and twisted magnetic flux tube. As long as the flux tube is untwisted, its curvature is concave toward the solar surface, and so it cannot support dense plasma against gravity. However, when it is twisted sufficiently, individual field lines may acquire a convex curvature near their summits and so provide support. Cool plasma then naturally tends to accumulate in such field line dips either by injection from below or by thermal condensation. As the tube is twisted up further or reconnection takes place below the prominence, one finds a transition from normal to inverse polarity. When the flux tube becomes too long or is twisted too much, it loses stability and its true magnetic geometry as an erupting prominence is revealed more clearly.

Subject headings: hydromagnetics — Sun: prominences

I. INTRODUCTION

One of the most fascinating and little understood areas of solar physics is the study of solar prominences, whose basic properties have been reviewed in books by Tandberg-Hanssen (1974), Jensen, Maltby, and Orrall (1979), Poland (1986), Ballester and Priest (1988), and Priest (1988). The two classical models for the global magnetic structure of solar prominences were proposed by Kippenhahn and Schluter (1957) and Kuperus and Raadu (1974) many years ago. In the Kippenhahn-Schluter geometry there is a simple coronal arcade, with normal (N) magnetic polarity: the magnetic field lines go up from the photosphere on one side of the prominence, pass through the prominence horizontally, and go back down to the photosphere on the other side. The Kuperus-Raadu geometry, on the other hand, has inverse (I) magnetic polarity: the magnetic field passes through the prominence in the opposite (or inverse) direction to the field lines below, and in some models it is associated with an X-type magnetic neutral point below the prominence. Observations of magnetic fields in prominences at the limb by Leroy (1989) have shown that large quiescent prominences at high latitudes possess I magnetic polarity, whereas smaller quiescent prominences at lower latitudes close to the active-region belts possess N magnetic polarity.

These classical models were proposed many years ago and are now believed to be unsatisfactory for a variety of reasons. In both cases a two-dimensional model is set up in a plane perpendicular to the prominence axis. Then, almost as an afterthought, an extra magnetic field component is added along the prominence, and yet observations show this component to be the dominant one since the field is inclined at typically only 20° to the axis. Furthermore, there are difficulties with the notion of the formation of a Kippenhahn-Schluter prominence by thermal condensation in a coronal arcade. One could argue that a highly sheared arcade is most favorable for condensation if the field line lengths need to exceed a critical value before condensation instability occurs, but why should there not then be the occasional very wide and unsheared arcade containing a prominence? Also, coronal arcades naturally tend to possess summits with a concave curvature toward the solar surface, and so cooling plasma would tend to drain away from the summit before it can accumulate (§ III). Similar difficulties apply to Kippenhahn-Schluter formation by injection from below. If it occurs in a highly sheared arcade, why should it not also work in an unsheared arcade without a strong field component along the prominence axis? Surely cool plasma is more likely to fall back down to the chromosphere than create a substantial dip in the field to support further material. Kuperus-Raadu models suffer from a serious problem of how to create a current of the required sign (Anzer 1988), since the effect of gravity during the formation naturally tends to produce one of the opposite sign corresponding to normal polarity. Furthermore, Anzer (1985) has shown that the self-pinching of a Kuperus-Raadu prominence sheet tends to create an unwanted downward force in the upper part of the sheet. Also there is not enough mass in the closed-field region to form a substantial prominence through condensation and chromospheric injection is ruled out by the field geometry.

The prominence model we are proposing is essentially three-dimensional: it is clear that the third component of the magnetic field (i.e., along the prominence axis) is crucial to the very existence of a prominence and so should play an important part in a prominence model. We suggest that when a large-scale curved magnetic flux tube (Fig. 1) is twisted enough, field lines within the tube may acquire locally a favorable upward curvature to provide support against gravity. Figure 2 sketches the evolution of such a flux tube as its twist increases. Twisting motions of various kinds have been well observed in prominences (Schmieder, Raadu, and Malherbe 1985; Schmieder *et al.* 1988; Mein and Schmieder 1988), and active-region prominences are well-known to occur along velocity shears (Harvey and Harvey 1980). Section II calculates the critical twist (Φ_{crit}) for prominence formation as a function of the summit altitude (h) and minor radius (a) of the flux tube. It also shows how the dip near the summit of a typical field line increases in size as the tube is twisted further beyond Φ_{crit}. The flux tube then becomes receptive to prominence formation either by condensation or injection, provided further conditions on the flux-tube length or injection speed are met, as outlined in § III. Section IV presents a local model for a prominence sheet supported within the flux tube, while § V outlines reasons for prominence eruption, and § VI concludes by sum-

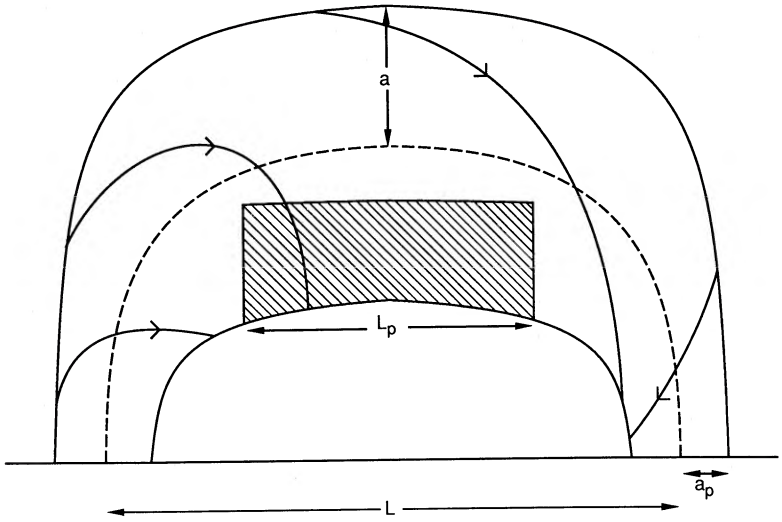

FIG. 1*a*

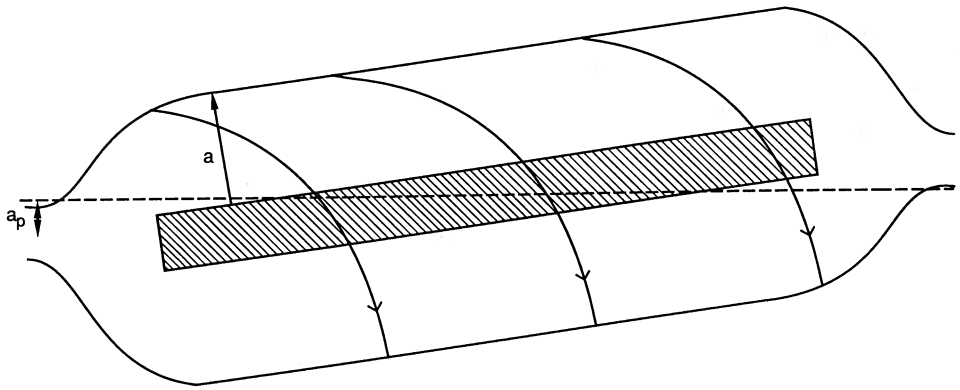

FIG. 1*b*

FIG. 1.—Large-scale twisted flux tube with footpoint separation L and minor radius a. The length of the prominence is L_p, where favorable curvature for formation exists. (*a*) From the side. (*b*) From above. (*c*) Cylindrical coordinate system (R, φ, Z) for a twisted flux tube with the Z-axis out of the plane of the figure. R_0 is the major radius about which twisting occurs. (*d*) The local coordinate system (r, θ) of the twisted flux tube of minor radius a in a plane perpendicular to (*a*).

marizing the properties and observational consequences of the model. It does not suffer from the difficulties raised by Anzer (1985, 1988) for the Kuperus-Raadu model, since the current is produced by condensation modifications to the basic flux-tube current which is in turn created by footpoint twisting motions. Furthermore, the force in the current sheet is everywhere upward (§ IV), and the mass can be supplied partly from the corona and partly along the helical field lines from the chromosphere, either by injection or by condensation-induced sucking.

II. CRITICAL TWIST FOR LOCAL SUPPORT

The purpose of this section is to illustrate how a twisted magnetic flux tube can have the correct curvature to support a coronal condensation. We set up a simple model of a twisted flux tube that illustrates how twisting photospheric motions produce magnetic configurations that can provide the necessary magnetic dip within which a condensation may form. We expect the flux tube to narrow where it reaches the solar surface, so that the flux comes from an area of radius a_p much less than the tube radius (a) in the corona (Fig. 1*a*–1*b*), but we shall neglect such a necking in this preliminary model.

Consider for illustration a potential field

$$\boldsymbol{B} = \frac{B_{\phi 0}}{R}\,\boldsymbol{e}_{\phi}\,,$$

where the cylindrical coordinate system (R, φ, Z) is shown in Figure 1*c*. Assume that circular twisting motions are centered about the major radius R_0 with a maximum minor radius a. The inverse aspect ratio, $a/R_0 = \epsilon$, is assumed much smaller than unity, and the field is expanded in powers of ϵ, with only the leading contributions retained.

If the flux surfaces are circular in cross section, to leading order the field components B_θ and RB_ϕ are just functions of r, and the relationship between the cylindrical and local coordinate systems is given by

$$R = R_0\left[1 - \frac{\epsilon r}{a}\cos\theta + O(\epsilon^2)\right],$$
$$Z = R_0\left[\frac{\epsilon r}{a}\sin\theta + O(\epsilon^2)\right], \tag{2.1}$$

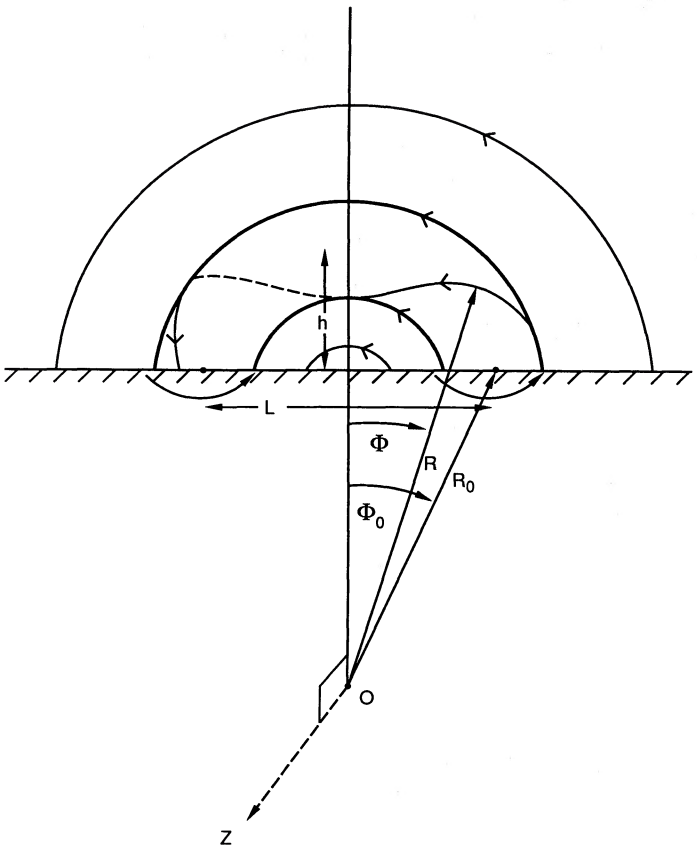

FIG. 1c

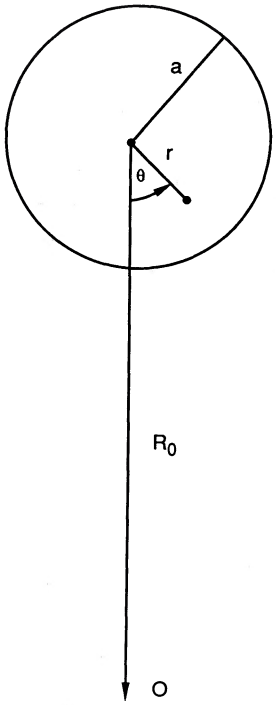

FIG. 1d

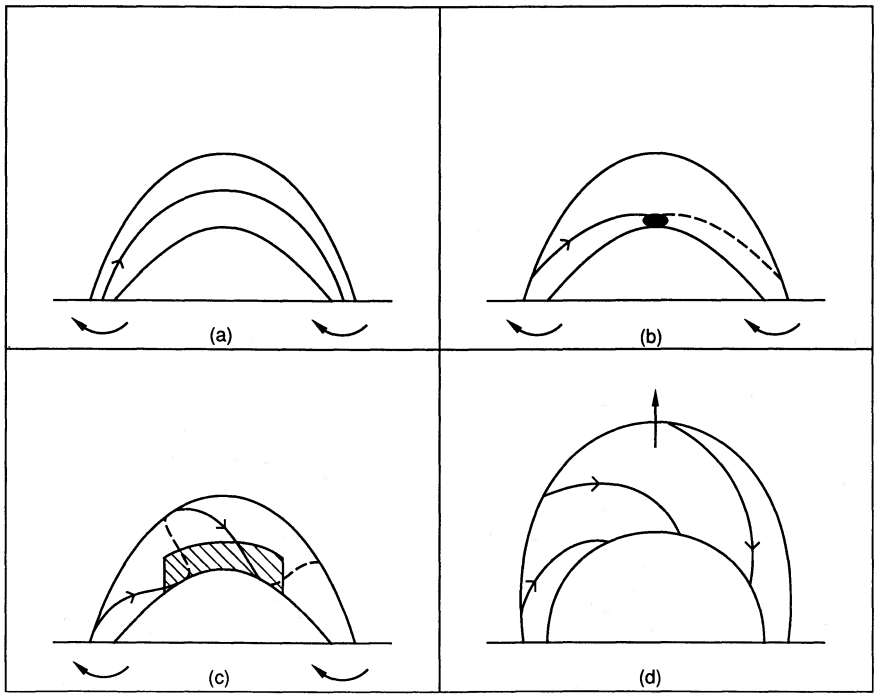

FIG. 2.—The evolution of a large flux tube as its twist increases. (*a*) No twist. (*b*) Critical twist Θ_{crit} for prominence formation to start at the tube summit. (*c*) Larger twist, with the prominence extending along the length L_p where curvature is favorable for support. (*d*) Such a large twist that the prominence erupts.

and

$$\frac{r}{a} = \frac{1}{\epsilon}\left[\left(\frac{R}{R_0} - 1\right)^2 + \left(\frac{Z}{R_0}\right)^2\right]^{1/2} + O(1)\,,$$
$$\theta = \tan^{-1}\left(\frac{Z/R_0}{1 - R/R_0}\right) + O(\epsilon)\,. \tag{2.2}$$

The magnetic field is then

$$\boldsymbol{B} = \begin{cases} (B_R,\, B_\phi,\, B_Z) + O(\epsilon)\,, & r \le a\,, \\ \left(0,\, \dfrac{B_{\phi 0}}{R}\,,\, 0\right), & r \ge a\,, \end{cases}$$

where

$$B_R = B_\theta(r)\sin\theta \quad r \le a\,, \tag{2.3}$$

$$B_\phi = \frac{g(r)}{R} \qquad r \le a\,, \tag{2.4}$$

$$B_Z = B_\theta(r)\cos\theta \quad r \le a\,. \tag{2.5}$$

To satisfy continuity of total pressure at $r = a$, $B_{\phi 0} = g(a)$ and $B_\theta(a) = 0$ (see Lothian and Hood 1988).

Using the definitions of B_R and B_Z, along with equation (2.1), it is easily verified that the leading contributions satisfy $\nabla \cdot \boldsymbol{B} = 0$. Equilibrium is obtained if the Lorenz force vanishes; to leading order this becomes the usual straight-cylinder equation:

$$\frac{B_\theta}{r}(rB_\theta)' + \frac{gg'}{R^2} = 0\,. \tag{2.6}$$

The equation of a field line is determined by solving

$$\frac{r\,d\theta}{B_\theta} = \frac{R\,d\phi}{B_\phi}\,,$$

and integrating gives the leading order contribution as

$$\phi = \frac{rg}{B_\theta R_0^2}\,\theta + \text{constant}\,. \tag{2.7}$$

Before proceeding, it is useful to express R_0 in terms of physically more useful quantities, namely the footpoint separation (L) and vertical height (h) of the flux tube. From Figure 1*c*,

$$R_0 = \frac{L(1 + \alpha^2)}{4\alpha}\,, \tag{2.8}$$

and

$$\phi_0 = \tan^{-1}\frac{2\alpha}{1 - \alpha^2} = \sin^{-1}\frac{2\alpha}{1 + \alpha^2}\,, \tag{2.9}$$

where $\alpha = 2h/L$ and the feet of the flux tube subtend angles $\phi = \pm\phi_0$. The inverse aspect ratio ($\epsilon = a/R_0$) can be expressed in terms of a, h, and L by, for example,

$$\epsilon = \frac{4\alpha}{1 + \alpha^2}\,\frac{a}{L}\,. \tag{2.10}$$

Now, using equation (2.7), the angle, Θ, through which a field line is twisted in passing from one end of the flux tube to the other is simply

$$\Theta(r) = 2R_0\phi_0\,\frac{R_0 B_\theta}{rg} = \frac{2R_0\phi_0}{\epsilon}\,\frac{B_\theta}{r/ag}\,, \tag{2.11}$$

and so, after using equation (2.11), the field line equation (2.7) may be rewritten as

$$\phi = \frac{2\phi_0}{\Theta}\,\theta + \text{constant}\,. \tag{2.12}$$

In order to understand how twisting a flux tube can provide a suitable dip in the magnetic field to enable a condensation to form, we must study the vertical field component, namely,

$$\begin{aligned} B_{\text{vert}} &= B_\phi \sin\phi - B_R\cos\phi \\ &= \frac{g}{R_0}\left[\sin\phi - \frac{R_0 B_\theta(r)}{g}\sin\theta\cos\phi\right] \\ &= \frac{g}{R_0}\left[\sin\phi - \frac{r}{R_0}\,\frac{\Theta}{2\phi_0}\sin\theta\cos\phi\right], \end{aligned} \tag{2.13}$$

where ϕ and θ are related by equations (2.12) and (2.11) has been used. The first field line that produces a dip is the one passing through $\theta = 0$ at $\phi = 0$, i.e. the lowest point at the top of the arcade. Thus, for such a field line the constant in equation (2.12) is zero. Expanding equation (2.13) about $\theta = 0$, $\phi = 0$, and using equation (2.12) gives the critical twist (from $dB_{\text{vert}}/d\phi = 0$) for the formation of a dip as

$$\Theta_{\text{crit}} = 2\phi_0\,\frac{B_\phi}{B_\theta} = 2\phi_0\left(\frac{R_0}{r}\right)^{1/2} = 2\phi_0\left(\frac{a}{\epsilon r}\right)^{1/2}. \tag{2.14}$$

For example, taking $r/a = 0.5$, $a/L = 0.05$, $h/L = 0.1$ gives $\phi_0 = 0.395$, $\epsilon = 0.038$, and $\Theta_{\text{crit}} = 1.8\pi$, which is just less than one revolution. On the other hand, a high flux tube in the shape of half a torus with $h/L = 0.5$ gives $\phi_0 = \pi/2$, $\epsilon = 0.1$, and $\Theta_{\text{crit}} = 4.5\pi$, just over two revolutions. Incidently, it is interesting to note that the result (2.14) follows from the definition $\Theta = 2R_0\phi_0 B_\theta/(rB_\phi)$ and the condition $B_\theta^2/r = B_\phi^2/R_0$ that the magnetic tensions due to B_θ and B_ϕ be equal.

Figure 3*a* shows how Θ_{crit} varies with the inverse aspect ratio (ϵ). The smaller the ϵ value, the larger the twist must be to produce a dip for fixed ϕ_0. If ϵ and the footpoint separation (L) are held fixed, then the lower the loop height (decreasing α and hence ϕ_0), the smaller the critical twist must be. Figure 3*a* gives a universal curve for Θ_{crit}, but the way it varies with h/L and a/L is also shown in Figure 3*b*.

As Θ is increased beyond the critical value (Θ_{crit}), the length (L_p) of the dip increases, as shown in Figure 4*a*. It is calculated by assuming that cool prominence material will drain to the bottom of the dip. Tracing out the position of minimum dip from B_{vert} vanishing, for different field lines, on the same flux surface, defines the initial length of the newly formed prominence. The maximum extent of the prominence is given by

$$\tan\phi_{\max} = \frac{r}{R_0}\,\frac{\Theta}{2\phi_0} \quad \text{and} \quad \theta = \frac{\pi}{2}\,, \tag{2.15}$$

and the length L_p is given approximately by

$$\frac{L_p}{L} = \frac{\sin\phi_{\max}}{\sin\phi_0}$$

since the prominence lies at a small angle to the torus axis.

Finally, the shape of a field line projected onto the R-ϕ plane is shown in Figure 4*b* as the footpoints are twisted. All these field lines pass through $\theta = 0$, $\phi = 0$, and the appearance of a dip is clearly seen. It should be noted that our estimates here are based on the thin torus approximation, whereas the true

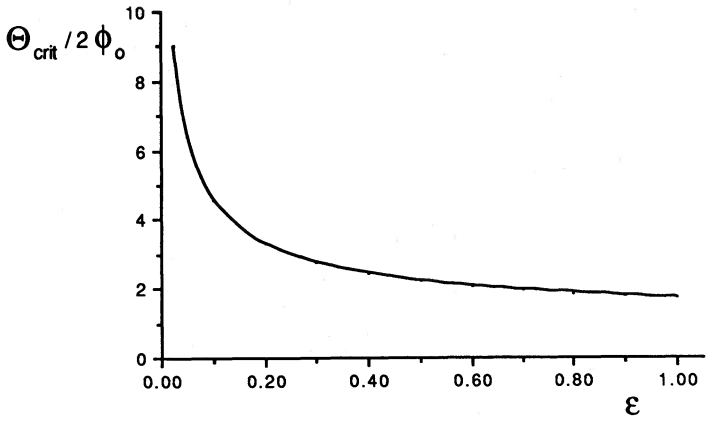

FIG. 3a

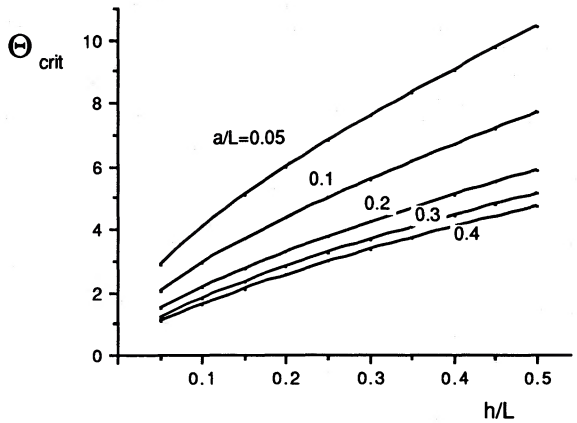

FIG. 3b

FIG. 3.—(*a*) The critical twist (Θ_{crit}) at a radius $r = 0.5a$ for the formation of a dip, measured in units of $2_{\phi 0}$, as a function of the inverse aspect ratio $\epsilon = a/R_0 = 8(a/L)(h/L)/(1 + 4h^2/L^2)$. $2_{\phi 0}$ is the angle subtended by the feet of the flux tube at its large-scale center of curvature. (*b*) The critical twist (Θ_{crit}) as a function of the flux-tube height (h) and minor radius (a), where L is the footpoint separation.

geometry is closer to that sketched in Figure 1. Therefore the estimates of this section are to be taken with some caution, although the general behavior should be represented properly. A more complete model would include a zeroth-order axial field to align the magnetic field with the polarity inversion (or "neutral") line. However, this added complication will not change the basic conclusion that twisting up a flux loop can indeed produce the correct curvature for prominence formation.

III. PROMINENCE FORMATION

Cool solar prominences could be produced through the process of condensation of coronal material. Coronal plasma can cool on the time scale of radiative losses; for typical coronal parameters ($n = 10^{14}$ m^{-3}, $T = 2 \times 10^6$ K) this is $\sim 10^5$ s (e.g., Priest 1982, p. 278). If the magnetic field in the region of condensation has convex curvature, then the cold material will fall down along the magnetic field. The free-fall time for a height of 30,000 km is 500 s. Because of the inclination of the field with respect to the vertical the actual time scale will be somewhat larger, but still much shorter than the cooling time. This implies that the material will fall down before it can cool efficiently. This leaking can be prevented by the existence of a dip in the magnetic field. The condensation itself cannot in practice produce the dip as the following estimates will show. Suppose that coronal material with density $n = 10^{14}$ m^{-3} and a width of 30,000 km condenses into a narrow sheet, then a gravitational force arises which has a surface density

$$F = \rho\, dg \approx 10^{-3} \text{ kg m}^{-1} \text{ s}^{-2} \text{ (or } 10^{-2} \text{ in cgs)} . \quad (3.1)$$

This force can be balanced by magnetic tension. A magnetic field which has a horizontal strength B_h and a jump in the vertical component $[B_z]$ produces a tension force

$$F_t = \frac{2}{\mu} B_h [B_z] . \quad (3.2)$$

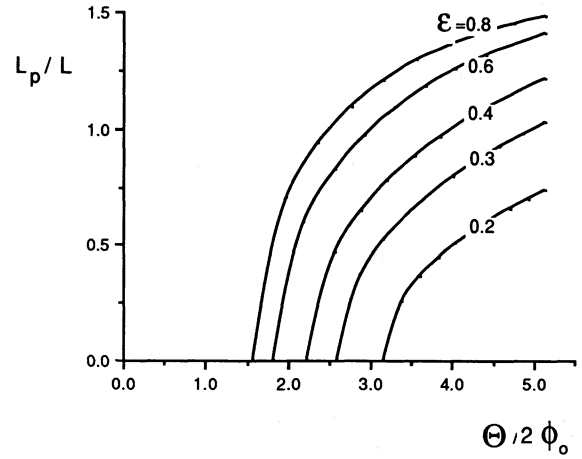

FIG. 4a

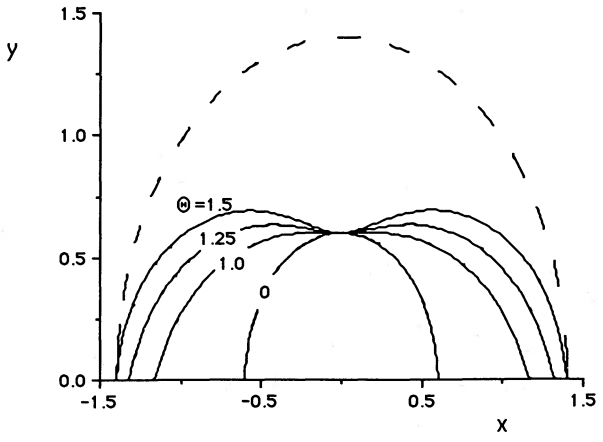

FIG. 4b

FIG. 4.—(*a*) The length (L_p) of the dip as a function of flux-tube twist (Θ) for several values of the aspect ratio ($\epsilon = a/R_0$) and $h/L = 0.15$ at a radius $r = 0.5a$. (*b*) The projections of a field line on the R-ϕ plane as it is twisted up by photospheric footpoint motions for several values of twist (Θ). Here $h/L = 0.2$, $\epsilon = 0.8$, and $r/a = 0.5$. ($\Theta = 1.5$ corresponds to about one-quarter of a turn.)

For $B_h = 5$ G equilibrium is obtained with $[B_z] = 10^{-2}$ G or $B_z^+ = -B_z^- = 5 \times 10^{-3}$ G. Therefore this sagging effect can be completely neglected.

We conclude from this that there must be a preexisting dip in the magnetic field of the prominence region (see An *et al.* 1988, who find that formation by injection can only work when the plasma beta is of order unity or greater). One may speculate that such dips can be formed in magnetic arcades if they are sheared in a special way. But what kind of shear function will produce dips is not known at present. Here we want to follow the picture of twisted flux tubes outlined in the preceding section. Such a flux tube can acquire regions where the field lines are curved upward if the twist is sufficiently large. Since our model is based on a single very large flux tube, the necessary twisting motion has to occur on a large geometrical scale and over long periods. A prime candidate for such a twisting action is the rotational flow due to Coriolis forces.

We assume that the magnetic field of the flux tube is anchored in the outer parts of a supergranule. In these cells one observes systematic flows from the cell center to the boundary. This flow will be diverted by the Coriolis force. For order-of-magnitude estimates we use a simple model described by Hide (1978). It has a radial outflow between the two cylinders $r = r_1$ and $r = r_2$, with

$$v_r = v_0 \frac{r_2}{r} . \tag{3.3}$$

This then leads to an azimuthal velocity given by

$$v_\varphi = \Omega\left\{-r + \frac{1}{r_2^{s+2} - r_1^{s+2}}\left[\frac{r_2^2 r_1^2 (r_2^s - r_1^s)}{r}\right] + (r_2^2 - r_1^2) r^{s+1}\right\} . \tag{3.4}$$

The exponent s is given by

$$s = \frac{r_2 v_0}{\nu} , \tag{3.5}$$

with ν being the viscosity coefficient. For a typical supergranule one has $v_0 = 1$ km s^{-1} and $r_2 = 15{,}000$ km; we also take an eddy viscosity $\nu_e = 10^9$ m^2 s^{-1} (10^{13} in cgs); e.g., Gilman (1976) gives $\nu_e \approx 10^{12}$–10^{14} cgs. This gives $s \approx 15$, and from Figure 5 of Hide one obtains a maximum value of

$$v_\phi = 0.8 \Omega r_2 . \tag{3.6}$$

The time for one revolution can be estimated as

$$\tau = \frac{2\pi r_2}{v_\phi} \approx \frac{2\pi}{0.8\Omega_0} , \tag{3.7}$$

which amounts to 3×10^6 s or 35 days. This shows that the mechanism is efficient in producing twisted flux tubes. It is possible that the same mechanism also works on the larger scale of giant cells. By comparison, the mean lifetime of high-latitude quiescent prominences is 140 days, and polarity inversion lines last even longer.

Next we want to discuss the orientation of the field with respect to the dividing line of the underlying bipolar region. An untwisted flux tube will show a normal polarity (as in Kippenhahn-Schluter models), but as it gets stretched by the action of differential rotation the tube becomes more aligned and its normal field component weaker. The rotational motion described above has a clockwise sense in the northern hemisphere and a counterclockwise sense in the southern hemisphere. In both hemispheres this twisting produces a field component opposite to the normal one in the lower part of the tube (Fig. 9). This means that as one increases the twist, the magnetic polarity in these parts of the tube can change from normal to inverse (i.e., Kuperus-Raadu type). An alternative cause for such a change in our model is reconnection below the flux tube due to convergent photospheric motions (Martin 1986; Van Ballegooijen and Martens 1989).

Differential rotation can also result in twisting—at least as long as it does not disintegrate the tube. Relative to a solid rotation one obtains an azimuthal velocity of

$$v_\phi = \Omega \frac{d \ln \Omega}{d\Theta} , \tag{3.8}$$

and a revolution time of

$$\tau = 2\pi\left(\Omega \frac{d \ln \Omega}{d\Theta}\right)^{-1} . \tag{3.9}$$

The observations give for mid-latitudes $d \ln \Omega / d\Theta \approx \frac{1}{6}$ leading to $\tau \approx 1.5 \times 10^7$ s. This is a factor of 5 larger than the time scale for the Coriolis flow and can therefore be neglected. It is, however, interesting to note that this rotation has the opposite sense of the one produced by the Coriolis effect.

Once such magnetic configurations with a dip are formed condensation can start. But to obtain equilibrium solutions which are cool at the top, hot over the coronal regional region, and cold again at the base an additional requirement has to be fulfilled: the flow of thermal energy by conduction into the prominence has to be sufficiently small. Hood and Anzer (1988) found that a spreading of the flux tube by a factor of 2 reduced the conduction enough so that prominence-type solutions are possible. Since our model needs an increase in tube radius by at least a factor of 3 for other (i.e., geometrical) reasons this condition will always be satisfied. Once the condensation has been established the accumulation of mass can be further enhanced by the siphon mechanism which was first proposed by Pikelner (1971).

These dip configurations could also be filled by an injection mechanism which brings in chromospheric material. But for this process to work special conditions have to be met. We discuss them for a configuration which has a dip at a distance h above the chromosphere and has a depth ΔZ which is small compared to h. We assume that material is injected from both sides of the loop. The velocities are v_{10} and v_{20} at the chromosphere and v_1 and v_2 at the bottom of the dip. For simplicity we assume that the densities are equal (i.e., $\rho_1 = \rho_2$). Then the material is trapped in the dip if

$$|v_1 - v_2| < \sqrt{2g\,\Delta Z} \tag{3.10}$$

holds. One also has

$$v_{10}^2 - v_1^2 = 2gh \quad \text{for } i = 1, 2 , \tag{3.11}$$

which gives

$$(v_{10} - v_{20})(v_{10} + v_{20}) = (v_1 - v_2)(v_1 + v_2) . \tag{3.12}$$

Then condition (3.10) leads to

$$|v_{10} - v_{20}| < \frac{v_1 + v_2}{v_{10} + v_{20}} \sqrt{2g\,\Delta Z} . \tag{3.13}$$

If we assume $v_{10}, v_{20} = O(2gh)^{1/2}$ and $v_1, v_2 = O(2g\,\Delta Z)^{1/2}$ the following rough estimate can be obtained

$$\frac{|v_{10} - v_{20}|}{v_{10}} < \frac{\Delta Z}{h}. \tag{3.14}$$

With $h = 30{,}000$ km and $\Delta Z = 3000$ km we find $|v_{10} - v_{20}|/v_{10} < 0.1$ and $|v_{10} - v_{20}| \leq 10$ km s^{-1}. This shows that the injection velocities have to be very well balanced in order to trap the material in the dip. But, on the other hand, we cannot completely rule out this mechanism on the basis of the above estimates.

IV. LOCAL SUPPORT IN A FLUX TUBE

In this section we show how a prominence, once formed, can be supported in a model flux tube by the azimuthal component (B_θ). In reality, especially in a low-beta quiescent prominence, the B_ϕ-component may be modified too, causing at first a flattening and later sometimes a dip in the ϕ-direction (see Velli and Hood 1989). Consider here, however, the magnetic field locally in the neighborhood of the prominence and neglect the large-scale curvature of the flux tube for simplicity. A more complete model would, of course, include such a curvature. For a force-free magnetic field which is independent of z, the distance along the prominence, the magnetic field components may be written (e.g., Low 1982; Hu, Hu, and Low 1983) in terms of a flux function (A) as

$$(B_r, B_\theta, B_z) = \left[\frac{1}{r}\frac{\partial A}{\partial \theta}, -\frac{\partial A}{\partial r}, B_z(A)\right], \tag{4.1}$$

where A is the solution of

$$\nabla^2 A + \frac{d}{dA}\left(\frac{1}{2}B_z^2\right) = 0 \tag{4.2}$$

once the functional form of B_z is prescribed. Note that here z is measured along the prominence, whereas in § II Z was normal to the plane of Figure 1*c*.

a) A Twisted and Confined Flux Tube

Now consider first a cylindrically symmetric flux tube (Fig. 5*a*) such as may exist before the prominence forms. It has only components $B_\theta(r)$ and $B_z(r)$, which depend on the radial distance (r) from the axis alone and which are related by

$$O = \frac{d}{dr}\left(\frac{B_\theta^2 + B_z^2}{2}\right) + \frac{B_\theta^2}{r}.$$

For example, consider for illustration fields of the form

$$B_\theta = \frac{B_0}{\sqrt{2}}\frac{r}{l}, \quad B_z = B_0\left(1 - \frac{r^2}{l^2}\right)^{1/2}, \quad 0 \leq r \leq a \tag{4.3}$$

which possess three parameters B_0, l, and a (the radius of the tube).

The magnetic flux ($2\pi F$) through the tube is given by

$$F = \int_0^a B_z r\,dr = \frac{B_0 l^2}{3}\left[1 - \left(1 - \frac{a^2}{l^2}\right)^{3/2}\right], \tag{4.4}$$

and the amount [$\Theta(r)$] by which a field line at radius r is twisted about the axis in going a distance L from one end of the tube to the other is

$$\Theta(r) \equiv \frac{LB_\theta}{rB_z} = \frac{L}{\sqrt{2}l(1 - r^2/l^2)^{1/2}}. \tag{4.5}$$

This may be written in terms of the axial twist $\Theta_0 = \Theta(0)$ as

$$\Theta(r) = \frac{\Theta_0}{(1 - r^2/l^2)^{1/2}}, \tag{4.6}$$

and the mean twist is

$$\Theta_m = \frac{1}{a}\int_0^a \Theta(r)dr = \frac{L}{\sqrt{2}a}\left(\sin^{-1}\frac{a}{l}\right). \tag{4.7}$$

Furthermore, from total pressure balance, the external total pressure (P_e) which can confine the flux tube is

$$P_e = \frac{B(a)^2}{2\mu} = \frac{B_0^2}{2\mu}\left(1 - \frac{a^2}{2l^2}\right). \tag{4.8}$$

Here P_e represents the sum of the magnetic plus plasma pressure in the external region, and under normal coronal conditions it is dominated by the magnetic pressure.

If l is set equal to a, so that the axial field (B_z) vanishes on the surface of the tube, and if the flux (F) and axial twist are given, then B_0 and a in equation (4.4) are given by

$$B_0 = \frac{3F_0}{a^2}, \quad a = \frac{L}{\sqrt{2\Theta_0}}. \tag{4.9}$$

Thus, if L and F are held fixed, as the tube is twisted up, so a decreases and B_0 increases.

A better model is to allow l to differ from a and use equations (4.4), (4.7), and (4.8) to deduce B_0, a, and l in terms of the flux (F), the mean twist (Θ_m), and the external pressure (p_e). Thus B_0 is given by equation (4.4) in terms of a, l, and F (where $l_0^4 = 9F^2/[4\mu P_e]$) as

$$B_0 = \frac{2l_0^2(\mu P_e)^{1/2}}{l^2[1 - (1 - a^2/l^2)^{3/2}]}, \tag{4.10}$$

while l and a are given in terms of Θ_m, P_e, and F from the coupled equations (4.7) and

$$l^4 = \frac{2l_0^4(1 - a^2/2l^2)}{[1 - (1 - a^2/l^2)^{3/2}]^2}. \tag{4.11}$$

Thus from equation (4.11) as a/l decreases from 1 to 0, so l increases from l_0 to infinity and a^4 approaches $(\frac{8}{9})^{1/4}l_0$. The resulting variations of l^4, a^4, and B_0 with Θ_m are shown in Figure 6. As the twist (Θ_m) increases from 0 up to $[\pi/2(2)^{1/2}]L/l_0$ so the magnetic length scale (l) decreases from infinity to l_0, while the tube radius (a) increases monotonically from $(\frac{8}{9})^{1/4}l_0$ to l_0 and the axial field (B_0) increases from zero to $2(\mu P_e)^{1/2}$. Also the scaling with flux (F) and external pressure (p_e) is contained in the parameter l_0

$$l_0 = \left(\frac{9F^2}{4\mu P_e}\right)^{1/4}.$$

We have here considered the simple force-free field of the form (4.3), but other forms such as "constant-alpha" or "uniform-twist" give similar results.

b) A Sheet Model within a Flux Tube

Suppose that the magnetic field in the neighborhood of a prominence is close to that of a cylindrically symmetric flux tube, so that the flux function has the form

$$A = A_0(r) + A_1(r, \theta), \tag{4.12}$$

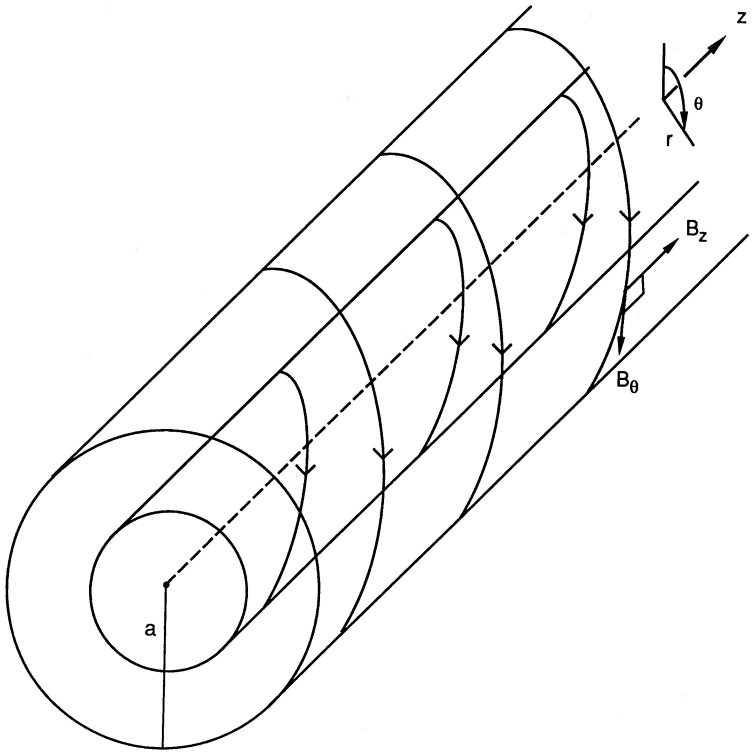

FIG. 5*a*

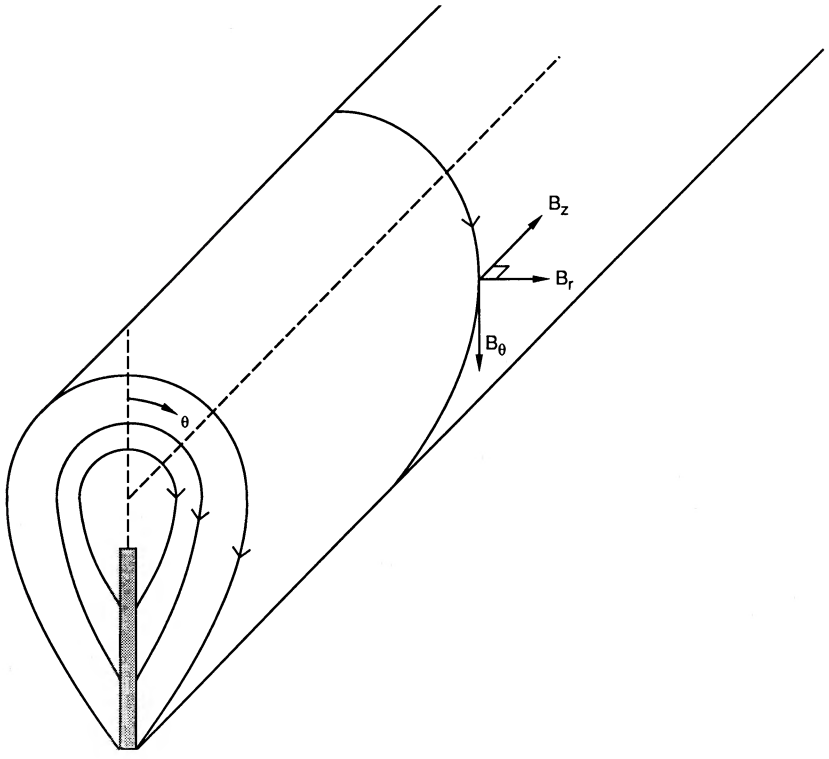

FIG. 5*b*

FIG. 5.—Notation for (*a*) a cylindrically symmetric flux and (*b*) a flux tube supporting a prominence sheet

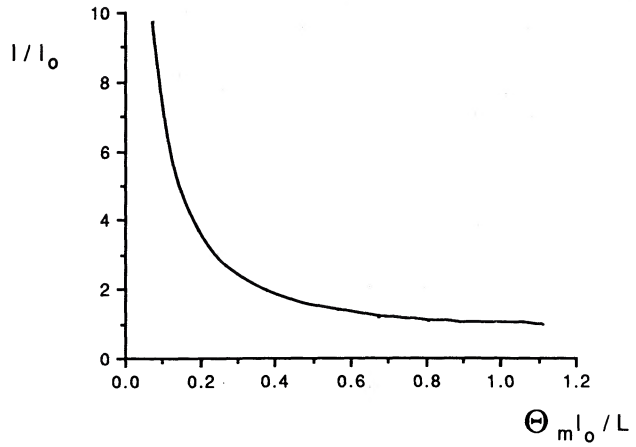

FIG. 6a

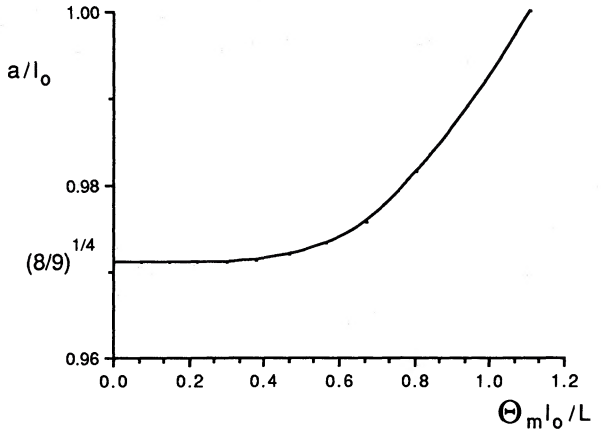

FIG. 6b

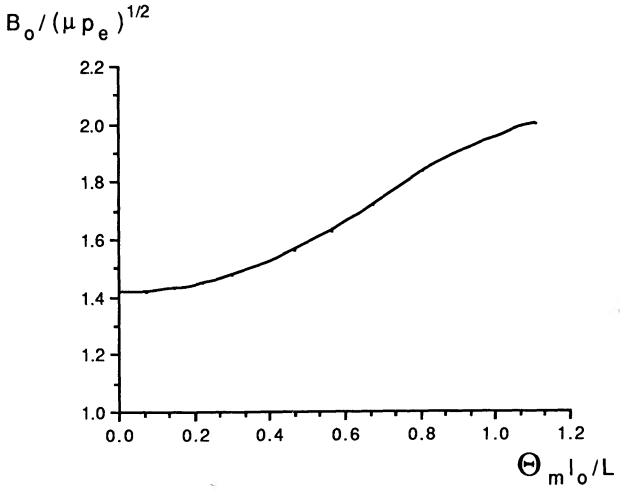

FIG. 6c

FIG. 6.—The variation with mean twist Θ_m of (*a*) the magnetic scale length l, (*b*) the radius a, and (*c*) the axial field strength B_0 of a flux tube, where $l_0^2 = 3F/(4\mu P_e)^{1/2}$ in terms of the axial flux (F) and external total pressure (P_e).

and

$$B_z = B_{0z}(r) + B_{1z}(r, \theta) .$$

In practice, the deformation produced by a fully formed prominence may be substantial, and so this approximation is appropriate for the initial condensation or for active region prominences where the magnetic field is very strong. A linearization about the cylindrically symmetric solution $[A_0(r)]$ then yields from (4.2) the basic equation which determines A_1, namely

$$\frac{dA_0}{dr}\left[\frac{1}{r}\frac{\partial}{\partial r}\left(r\frac{\partial A_1}{\partial r}\right)+\frac{1}{r^2}\frac{\partial^2 A_1}{\partial\theta^2}\right]-\frac{d}{dr}\left[\frac{1}{r}\frac{d}{dr}\left(r\frac{dA_0}{dr}\right)\right]A_1 = 0 . \tag{4.13}$$

Separable solutions to equation (4.13) may be sought of the form

$$A_1 = R(r)f(\theta) ,$$

for which

$$\frac{d^2 f}{d\theta^2} + K^2 f = 0 , \tag{4.14}$$

and

$$\frac{A_0'}{r}\frac{d}{dr}\left(r\frac{dR}{dr}\right)-\frac{d}{dr}\left[\frac{1}{r}\frac{d}{dr}\left(r\frac{dA_0}{dr}\right)\right]R = K^2\frac{A_0' R}{r^2} , \tag{4.15}$$

where K^2 is the separation constant, assumed here positive.

If the field lines are assumed symmetric about a vertical axis (as shown in Fig. 5*b*) and if θ is measured from the upward vertical, the boundary condition

$$B_r = \frac{1}{r}\frac{\partial A}{\partial\theta} = 0 \quad \text{at } \theta = 0$$

implies that

$$f = \epsilon \cos K\theta ,$$

where $\epsilon(\ll 1)$ is the linearization parameter.

In general, equation (4.15) can be integrated numerically, but for the particular form $A_0(r) = -B_0 r^2/(2\sqrt{2}l)$ corresponding to the field (4.3), it reduces to

$$r^2R'' + rR' - K^2R = 0 . \tag{4.16}$$

Solutions behaving like r^n have

$$n^2 = K^2 , \tag{4.17}$$

and the requirement that $n > 0$ so that A_1 has no singularity at $r = 0$ implies that we have to select the positive solution. The resulting field components are

$$\begin{aligned} B_{1r} &= Rf/r = -\epsilon K r^{K-1} \sin K\theta , \\ B_{1\theta} &= -dR/drf = -\epsilon K r^{K-1} \cos K\theta , \end{aligned} \tag{4.18}$$

for $-\pi < \theta < \pi$. In order that B_{1r} and $B_{1\theta}$ are well-behaved at $r = 0$ we need

$$K > 1 . \tag{4.19}$$

Another condition is that $B_{1r} > 0$ at $\theta \leq \pi$ so that there is an upward curvature at the prominence sheet ($\theta = \pi$) in order to provide magnetic support for the prominence against gravity, and this implies

$$\epsilon \sin K\pi < 0 . \tag{4.20}$$

When $\epsilon > 0$ this (and eq. [4.19]) implies that

$$1 < K < 2$$

(the fundamental solution). However, for $3/2 < K < 2$ one finds that $B_{1\theta} < 0$, and $B_{1\theta}(\sim r^{K-1})$ dominates $B_{0\theta}(\sim r)$ near $r = 0$, no matter how small ϵ is, so giving a downward Lorentz force. One thus has to exclude this region, and K is limited to $1 < K < 3/2$ in this case. For higher harmonics

$$2m - 1 < K < 2m , \quad m = 2, 3, \ldots .$$

The resulting variation of B_{1r} with θ and r and the magnetic field lines are shown in Figure 7. Now, locally within the

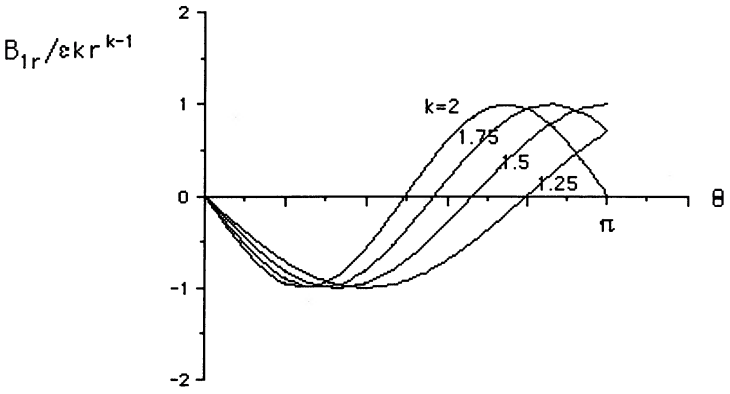

FIG. 7a

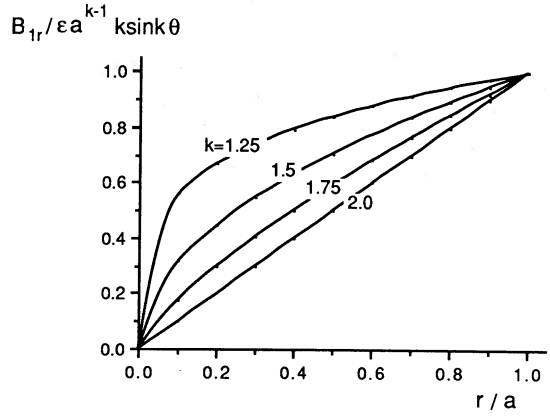

FIG. 7b

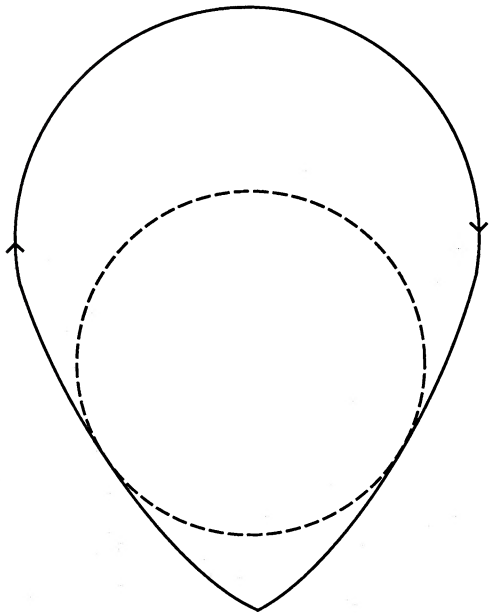

FIG. 7c

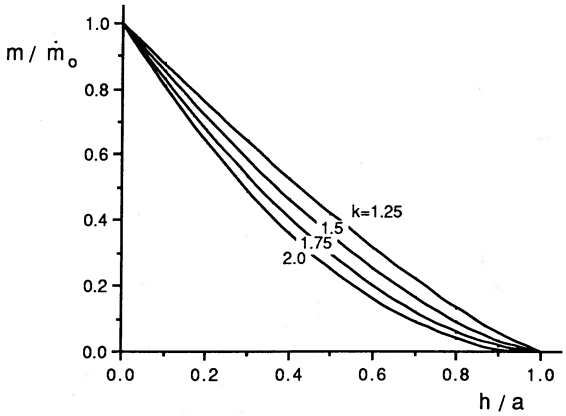

FIG. 7d

FIG. 7.—The variation with (*a*) θ and (*b*) r of the radial field component B_{1r} for several values of K between 1 and 2 and with $\epsilon > 0$. (*c*) A magnetic field line for $K = 1.5$ in a plane perpendicular to the flux-tube axis and $\epsilon = 0.5$. (*d*) The variation of prominence mass (m) with height $h = a - r$.

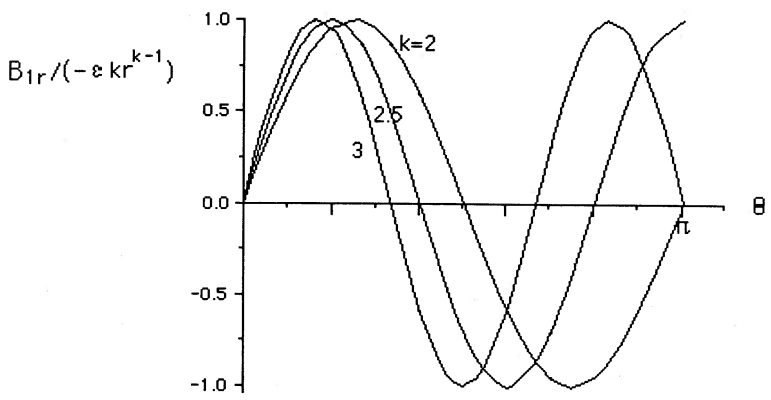

FIG. 8*a*

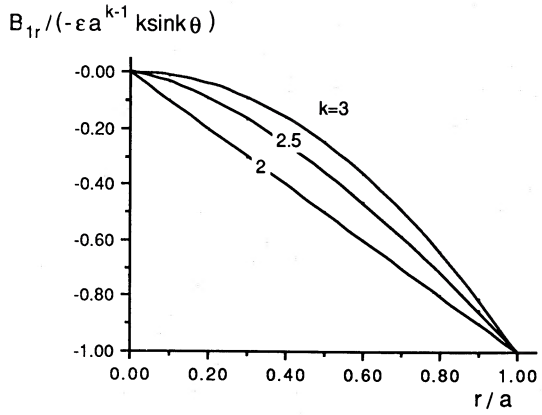

FIG. 8*b*

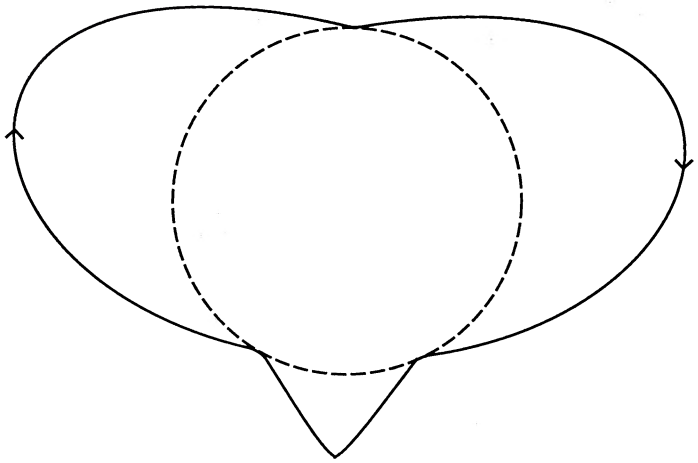

FIG. 8*c*

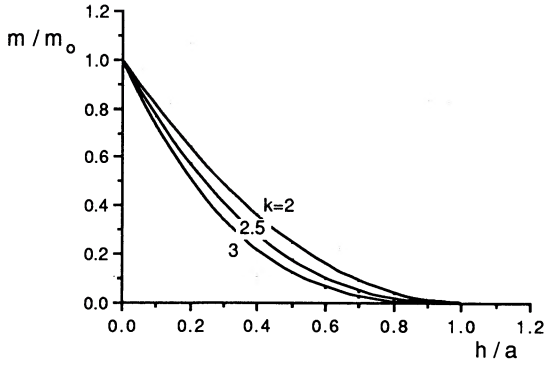

FIG. 8*d*

FIG. 8.—As for Fig. 7, but with $\epsilon < 0$ and values of K lying between 2 and 2. $K = 3$ for (*c*).

prominence we may assume a local balance

$$\rho g = j_z B_h$$

between gravity and the Lorentz force, and this may be integrated across the prominence (assumed so thin that the horizontal field component B_h is uniform) to give

$$mg = [B_{1r}]B_{0\theta}/\mu ,$$

where m is the prominence mass density per unit length integrated across the prominence, $[B_{1r}]$ is the jump in B_{1r} across the prominence from $\theta = \pi$ to $\theta = -\pi$, and $B_{0\theta} = B_0 r/(\sqrt{2}l)$ for the field (4.3). In other words,

$$m = m_0\left(\frac{r}{a}\right)^K , \qquad (4.21)$$

where

$$m_0 = -\sqrt{2}\epsilon K \sin (K\pi)B_0 a^K/(l\mu g) .$$

The variation of m with height (h) in the prominence is shown in Figure 7*d*. Since the condensing plasma is expected to drain down the field lines and occupy a narrow region only a scale height thick (based on the prominence temperature), the approximation of treating the prominence as a sheet is a good one (see Low 1981*a*).

When $\epsilon < 0$, condition (4.20) implies that

$$2m < K < 2m + 1, \quad m = 1, 2, \ldots ,$$

and in particular we show the variations of B_{1r} and prominence mass in Figure 8 for $2 < K < 3$. Here the curvature of the field lines in a section across the flux tube (Fig. 8*c*) is rather different than for Figure 7, since a field line starting from the top of the flux tube first moves out to a larger radius before (as in Fig. 7*c*) coming in to a minimum radius with a reversed curvature and then moving out near the prominence location.

V. DISCUSSION

a) Eruption

Most prominences erupt at some point in their lifetime but often reform in the same location, presumably because the basic magnetic mould and the velocity patterns which are necessary for prominences to exist are not completely destroyed. An eruption takes place somewhere on the Sun typically once every other day, and it usually produces (or is produced by) a coronal mass ejection. When an active-region prominence erupts, it generally creates a large two-ribbon flare.

During the eruption of a prominence it often has an appear-

ance suggestive of a twisted flux tube, which is therefore one of the main motivations for the present model. Indeed, it is, in view of this observation, surprising that a twisted flux tube nature has not been central to most previous models of their quiescent state. Since the large-scale twisting up of a flux tube is, we have argued, a likely cause of prominence formation, it is natural that as the twist continues the attainment of a second critical twist may cause an eruption. One should, however, be aware that observed structure giving the impression of helical twisting could also result from a system of oppositely inclined strands lying on both sides of a vertical sheet. In particular, filling a whole flux tube with cool dense material in equilibrium causes a theoretical problem, since in the upper part of such a tube the Lorentz force is not in the right direction to counteract gravity. Perhaps this is why it is only in the highly nonequilibrium state of prominence eruption that a flux-tube geometry is revealed.

Several analyses of prominence stability support this suggestion. First of all, a simple force-free magnetic arcade with shear but no twist (i.e., no magnetic island in a plane perpendicular to the arcade) is extremely difficult if not impossible to make ideally unstable (Hood and Priest 1980; Hood and Anzer 1987). However, when a magnetic island is present so that we have a large-scale flux tube with an overlying arcade, instability may result when either the twist is too great or the height of the prominence is too great or the width of the arcade is too large (Hood and Priest 1980; Birn and Schindler 1981; Einaudi and Van Hoven 1983; Hood 1983, 1984; Migliuolo and Cargill 1983; Low 1982). For a uniform-twist field, Hood and Priest (1980) showed that the stabilizing effect of photospheric line tying is to give a critical twist of 2.5π (i.e., greater than the Kruskal-Shafranov limit), whereas for a linear force-free field with an inversion Einaudi and Van Hoven (1983) obtained a higher value of 20π. If a typical critical twist for an eruption to occur is in the range 2.5π, to 20π, and is 2π say, for prominence formation, then the lifetime of a prominence (based on the estimates for twisting motions in § III) would be in the range 17 days to 310 days. As well as twisting, there may be spreading motions, for example, in the decay of a remnant active region which can lead to prominence eruption. Another possibility is that if the plasma pressure gradient becomes too large, an arcade may lose equilibrium (Zwingmann 1985) or go unstable (Hood 1986; Velli and Hood 1986; Cargill, Hood, and Migliuolo 1986). But this seems less likely since in general the solar corona is completely dominated by the presence of strong magnetic fields.

By analyzing the equilibrium of a magnetic flux tube under a balance between magnetic buoyancy and tension forces, it has been shown that the tube may lose equilibrium if the twist is too great or if the separation of the footpoints is too large, typically greater than a coronal scale height (Parker 1979; Low 1981*b*; Browning and Priest 1984, 1986; Wolfson 1982). As far as the latter possibility is concerned, perhaps if two neighboring tubes are joined together by reconnection they may create a longer tube which cannot be in equilibrium and so erupts. Furthermore, K. Harvey (private communication) has suggested that for active-region prominences the observed photospheric flow may not be fast enough to stretch out a long flux tube, so that instead it may be created by connecting together several small flux tubes. Indeed, the fascinating observations of Martin (1986) reveal many small regions of cancelling magnetic flux near prominence footpoints which are probably sites of reconnection submergence, as argued by Priest (1987) and Zwaan (1987). This process may also cause a change in polarity from normal to inverse.

Another model of the way prominence eruption may be initiated has been put forward by Demoulin and Priest (1989), based on an earlier qualitative model by Van Tend and Kuperus (1978) and an analysis by Amari and Aly (1989). Here the equilibrium of a twisted magnetic flux tube (treated as a line current) in a force-free arcade is calculated, and it is found that, when the twist (or current) is too great or the arcade shear is too large, the flux tube can no longer be in equilibrium and the imbalance of forces is such as to make it erupt. The actual eruption after losing equilibrium has been recently studied by Steele and Priest (1988), in which the eruption drives reconnection below the prominence and so allows the eruption to proceed faster than otherwise. Their analysis is a development of an earlier model by Anzer and Pneuman (1982) in which reconnection drove the eruption.

b) Formation and Twisting of the Flux Tube

How does the flux tube form? Malherbe and Priest (1983) and Priest (1987) have suggested that quiescent prominences lie along giant cell boundaries that separate unipolar regions. Differential rotation or shear at such boundaries (or fault lines) may then stretch out the arcade that arches over a boundary and create a long flux tube inclined at a small angle to the boundary. Shearing motions (Ambroz 1987) may, for example, occur at the boundary of the polar field and flux migrating toward it from lower latitudes. For active-region prominences, they may also be present near the edges of active regions or between neighboring active regions (see Harvey and Harvey 1980, who find all such prominences to lie along velocity shears).

Once the flux tube is stretched out, how is it twisted up in a systematic way that tends to produce normal polarity prominences at low latitudes and inverse polarity at high latitudes later in their lives as they drift towards the poles? Possible twisting mechanisms are shear gradients at giant cell boundaries, differential rotation or Coriolis forces in supergranules as flux is carried from cell centers and concentrated at cell junctions. The estimates of § III favor the Coriolis effect which can twist up the tube over times of 10–100 days. Another, less likely, possibility is that the flux tube emerges already twisted.

c) General Properties

An important topic of prominence physics which has been virtually ignored until recently is the nature of prominence feet. One possibility is that they represent local regions where so much plasma has accumulated that the flux tube sags down to the chromosphere. Alternatively, the lower boundary of the prominence (presumably the critical height for prominence formation) could vary in a three-dimensional model because of several effects: either the field line divergence may vary along the prominence, or the field may become more normal to the prominence axis (and so reduce the thermal shielding) or the transverse magnetic field may vary and so allow different amounts of sag. For example, Demoulin, Priest, and Anzer (1988) have suggested that prominences with normal polarity tend to have their feet at the centers of supergranules, while those with inverse polarity tend to have them located at supergranule boundaries.

Another neglected topic is the presence of fine vertical prominence threads, which may be caused by an interchange or resistive instability including thermal and gravitational

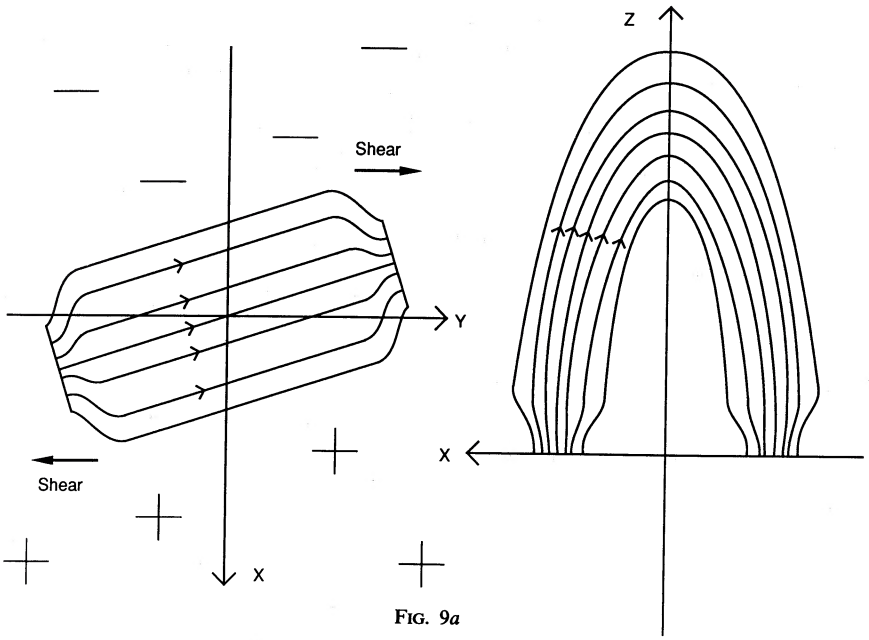

FIG. 9a

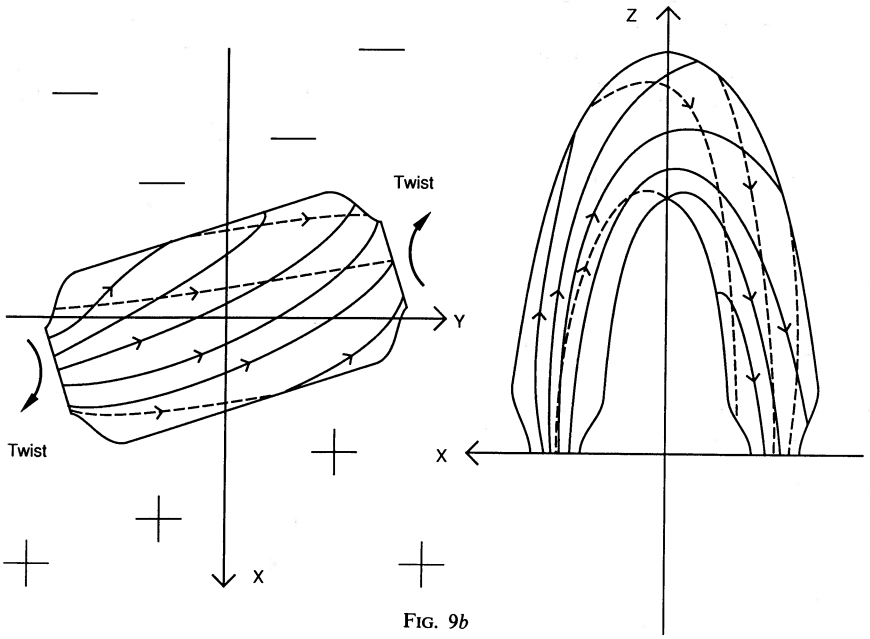

FIG. 9b

FIG. 9.—Long-term evolution of the magnetic flux tube within which a prominence forms, shown both from above (x-y plane) and in the xz-plane normal to the prominence sheet; i.e., looking along the prominence. (*a*) Shearing of a flux tube at a polarity inversion line (y-axis). (*b*) Twisting due to Coriolis forces produces a dip and a prominence with normal polarity. (*c*) Transition. (*d*) Increasing twist gives a prominence with inverse polarity. Field lines on the near side of the flux tube are shown solid, whereas those on the far side are dashed. (*e*) Evolution from normal to inverse polarity of a configuration including an ambient magnetic arcade in a section across the prominence.

effects. Alternatively, a local condensation may tend to communicate vertically as it sags and create dips on neighboring field lines above and below (Poland and Mariska 1988).

One observational consequence of our model is that the prominence axis should be inclined very slightly (Fig. 1*b*) to the polarity inversion line: for example, a source diameter ($2a_p$) of 4 Mm and a prominence length of 100 Mm implies an inclination angle of 2°. Another consequence is that the ends of the prominence should be anchored in magnetic sources and sinks at the photosphere.

Two possible long-term evolution sequences for prominences going from normal to inverse polarity as they migrate poleward have been considered by Hirayama (1985), but there are theoretical difficulties with them. In sequence A due to Pneuman, reconnection in going from (*b*) to (*c*) is most unlikely and in sequence B going from (*b*) to (*c*) by shearing and twisting

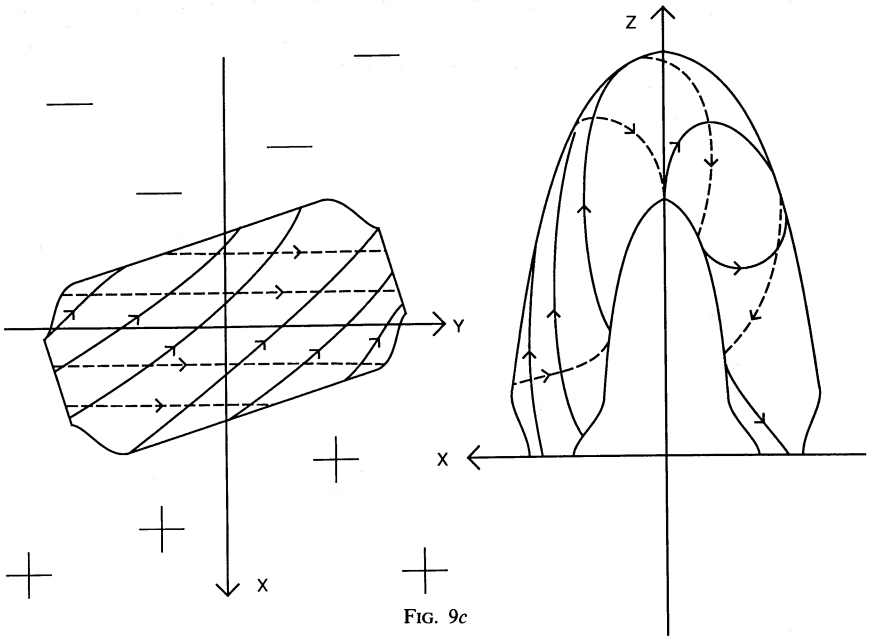

FIG. 9c

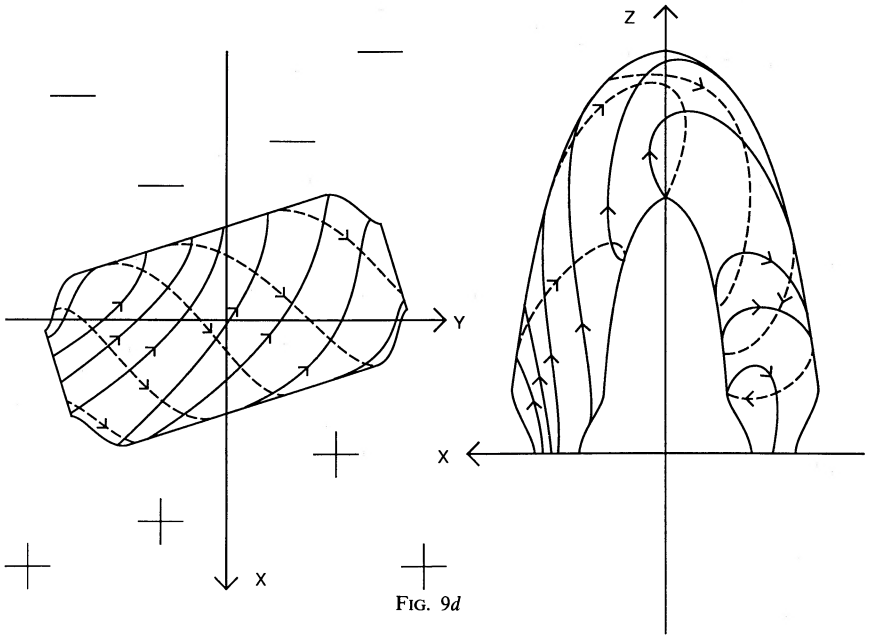

FIG. 9d

needs an unlikely rotation about the vertical axis of each magnetic plane of the configuration. We would like to suggest instead the evolution shown in Figure 9 as a natural consequence of shearing and twisting. As the flux tube is twisted up it first forms a prominence with N-polarity (Fig. 9*b*), passes through a transition (Fig. 9*c*) and then forms a prominence with I-polarity (Fig. 9*d*). Since the prominence is located at the dips in the field lines, it is inclined very slightly to the photospheric polarity inversion line, and so the inversion polarity relative to the prominence sheet will take place at a slightly different twist from the inversion relative to the polarity inversion line. Another point to notice is that the evolution from N-polarity to I-polarity can also result from reconnection below the flux tube.

Figure 9*e* shows the evolution from N- to I-polarity of a possible global magnetic field, including an ambient magnetic arcade, in the x-z plane across the prominence corresponding to Figures 9*b*–9*d*. As twisting continues, a cusp-type neutral point is formed, and the lower part of the prominence changes from N-polarity to I-polarity. The local configuration near the cusp may be modeled by a flux function $A = x^2 + y^3/3$ giving field components

$$(B_x, B_y) = (+y^2, -2x) ,$$

and a current density $j = -2(1 + y)/\mu$. As the twist continues, the cusp splits into a pair of O- and X-type neutral points with local flux functions $A = x^2 + y^2$ and $A = x^2 - y^2$, respectively,

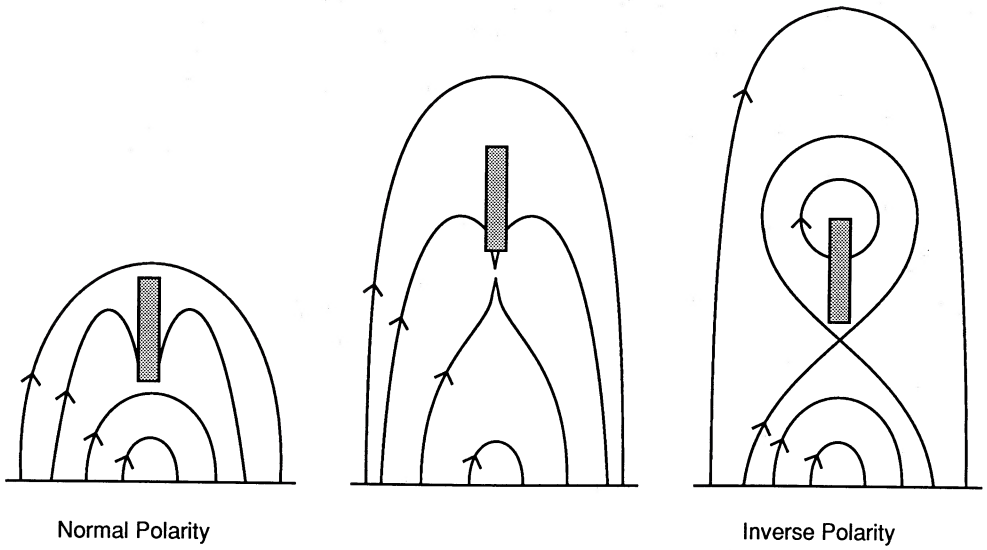

FIG. 9e

say. Prominence formation with I-polarity then becomes possible in the lower part of the magnetic island around the O-point. For a time both types of prominence may possibly coexist, but eventually when the magnetic island has grown substantially we have shown in the last sketch only a prominence with I-polarity.

When a prominence erupts it undergoes a metamorphosis and changes its appearance from a thin vertical sheet to a curved tube, although sometimes it looks like a twisted sheet. The eruptive process clearly disrupts and heats the prominence material allowing it to fill up parts of the erupting tube, whereas previously it was sitting quietly in potential wells at the bottoms of field line dips.

VI. SUMMARY

We have suggested that the stretching and twisting of a large magnetic flux tube naturally explains many observational features of quiescent solar prominences. The model is essentially three-dimensional. Twisting by Coriolis forces can create a dip in the flux tube when the twisted field component (B_θ) exceeds $(a/R_0)^{1/2}B_\phi$, where B_ϕ is the field component along the flux tube and a and R_0 are the minor and major radii of curvature of the tube. The presence of the dip can then allow the prominence to form by thermal condensation (if the criterion for radiative instability is satisfied) or by injection (for low-lying prominences when the injection speed is high enough). As a prominence migrates poleward and becomes more twisted or undergoes reconnection it passes from one of normal polarity to inverse polarity.

Other features which arise naturally are: the difference in polarity between low-latitude and high-latitude prominences; the braids (indicative of twist) seen in high-resolution pictures of active-region prominences before they erupt (Gaizauskas 1985; Jockers and Engvold 1975; House and Berger 1987); the twist seen in erupting prominences; the gradual spread along the polarity inversion line of a prominence as it develops (presumably as the twist increases and the length L_p where a dip exists increases).

The model which has been outlined in this paper will be worked out in more detail in future. It is hoped to consider in particular the process of formation and the prominence structure more precisely. Furthermore, one hopes that it may act as a stimulus for much more observational work in order to determine the properties and precise locations of feet, the detailed magnetic structure of a mature prominence and the way prominences are born, evolve, and eventually die.

We are extremely grateful to Sara Martin and Karen Harvey for helpful comments, to Hania Allen for computational assistance, to Jose-Luis Ballester for organizing the prominence workshop where these ideas were born, and to the UK Science and Engineering Research Council for financial support. U. A. thanks the Mathematical Sciences Department of St. Andrews for kind hospitality during his visit.

REFERENCES

Amari, T., and Aly, J. J. 1989, *Solar Phys.*, in press.
Ambroz, P. 1987, *Bull. Astr. Inst. Czech.*, **38**, 1.
An, C. H., Wu, S. T., Bao, J. J., and Seuss, S. T. 1988, in *Dynamics and Structure of Solar Prominences*, ed. J. L. Ballester and E. Priest (Palma Mallorca: Universitat de les Illes Balears), p. 89.
Anzer, U. 1985, in *Measurements of Solar Vector Magnetic Fields*, ed. M. J. Hagyard (NASA CP 2374), p. 101.
———. 1988, in *The Dynamics and Structure of Quiescent Solar Prominences*, ed. E. R. Priest (Dordrecht: Reidel), pp. 143–166.
Anzer, U., and Pneuman, G. W. 1982, *Solar Phys.*, **79**, 129.
Ballester, J. L., and Priest, E. R., eds. 1988, *Dynamics and Structure of Solar Prominences* (Palma Mallorca: Universitat de les Illes Balears).
Birn, J., and Schindler, K. 1981, in *Solar Flare MHD*, ed. E. R. Priest (New York: Gordon & Breach, pp. 337–378.
Browning, P. K., and Priest, E. R. 1984, *Solar Phys.*, **92**, 173.
———. 1986, *Solar Phys.*, **106**, 335.
Cargill, P. J., Hood, A. W., and Migliuolo, S. 1986, *Ap. J.*, **309**, 402.
Demoulin, P., and Priest, E. R. 1989, *Astr. Ap.*, **206**, 336.
Demoulin, P., Priest, E. R., and Anzer, U. 1989, *Astr. Ap.*, in press.
Einaudi, G., and Van Hoven, G. 1983, *Solar Phys.*, **88**, 163.
Gaizauskas, V. 1985, in *Proc. Kunming Workshop on Solar Physics and Interplanetary Travelling Phenomena*, ed. C. de Jager and C. Biao (Beijing: Science Press), p. 710.
Gilman, P. A. 1976, in *IAU Symposium 71, Basic Mechanisms of Solar Activity*, ed. V. Bumba and J. Kleczek (Dordrecht: Reidel), p. 207.
Harvey, K., and Harvey, J. 1980, in *Proc. Solar-Terrestrial Predictions*, Vol. 3, p. C-41.
Hide, R. 1978, in *Rotating Fluids in Geophysics*, ed. P. H. Roberts and A. M. Soward (London: Academic), pp. 1–28.
Hirayama, T. 1985, *Solar Phys.*, **100**, 415.

Hood, A. W. 1983, *Solar Phys.*, **87**, 279.
———. 1984, *Geophys. Ap. Fluid Dyn.*, **28**, 223.
———. 1986, *Solar Phys.*, **103**, 329.
Hood, A. W., and Anzer, U. 1987, *Solar Phys.*, **111**, 333.
Hood, A. W., and Priest, E. R. 1980, *Solar Phys.*, **66**, 113.
House, L., and Berger, M. 1987, *Ap. J.*, **323**, 406.
Hu, W. R., Hu, Y. Q., and Low, B. C. 1983, *Solar Phys.*, **83**, 195.
Jensen, E., Maltby, P., and Orrall, F. Q. 1979, ed., of *IAU Colloquium 44, Physics of Solar Prominences* (Oslo: Servicesentrale), p. 375.
Jockers, K., and Engvold, O. 1975, *Solar Phys.*, **44**, 429.
Kippenhahn, R., and Schluter, A. 1957, *Zs. Ap.*, **43**, 36.
Kuperus, M., and Raadu, M. A. 1974, *Ap. J.*, **31**, 189.
Leroy, B. 1989, in *Dynamics and Structure of Quiescent Solar Prominences*, ed. E. R. Priest (Dordrecht: Reidel), chap. 4.
Lothian, R., and Hood, A. W. 1989, *Solar Phys.*, in press.
Low, B. C. 1981*a*, *Ap. J.*, **246**, 538.
———. 1981*b*, *Ap. J.*, **251**, 352.
———. 1982, *Rev. Geophys. Space Phys.*, **20**, 145.
Malherbe, J., and Priest, E. R. 1983, *Astr. Ap.*, **123**, 80.
Martin, S. F. 1986, in *Coronal and Prominence Plasmas*, ed. A. I. Poland (NASA CP 2442), p. 73.
Mein, P., and Schmieder, B. 1988, in *Dynamics and Structure of Solar Prominences*, ed. J. L. Ballester and E. R. Priest (Palma de Mallorca: Universitat de les Illes Balears).
Migliuolo, S., and Cargill, P. J. 1983, *Ap. J.*, **271**, 820.
Parker, E. N. 1979, *Cosmical Magnetic Fields* (Oxford: Oxford University Press).
Pikelner, S. B. 1971, *Solar Phys.*, **17**, 44.
Poland, A. I., ed. 1986, *Coronal and Prominence Plasmas* (NASA CP 2442).
Poland, A. I., and Mariska, J. T. 1988, preprint.
Priest, E. R., ed. 1982, *Solar Flare MHD* (Dordrecht: Reidel).
———. 1987, in *The Role of Fine-Scale Magnetic Fields on the Structure of the Solar Atmosphere*, ed. E. H. Schroter, M. Vazquez, and A. A. Wyller (Cambridge: Cambridge University Press) p. 297.
———. 1988, ed. *The Dynamics and Structure of Quiescent Solar Prominences* (Dordrecht: Reidel).
Schmieder, B., Raadu, M. A., and Malherbe, J. 1985, *Astr. Ap.*, **142**, 249.
Schmieder, B., Thompson, A., Demoulin, P., and Poland, A. 1988, *Astr. Ap.*, **197**, 281.
Steele, C. D. S., and Priest, E. R. 1989, *Solar Phys.*, **119**, 157.
Tandberg-Hanssen, E. 1974, *Solar Prominences* (Dordrecht: Reidel).
Van Ballegooijen, A., and Martens, P. 1989, preprint.
Van Tend, W., and Kuperus, M. 1978, *Solar Phys.*, **59**, 115.
Velli, M., and Hood, A. W. 1986, *Solar Phys.*, **106**, 353.
Wolfson, R. 1982, *Ap. J.*, **255**, 174.
Zwaan, C. 1987, *Ann. Rev. Astr. Ap.*, **25**, 83.
Zwingmann, W. 1987, *Solar Phys.*, **111**, 309.

U. ANZER: Max-Planck-Institut für Astrophysik, Karl-Schwarzschild Strasse 1, D-8046 Garching bei Muchen, West Germany

A. W. HOOD and E. R. PRIEST: Mathematical Sciences Department, University of St. Andrews, St. Andrews, KY16 9SS, Scotland, UK